This article has been accepted for publication in a future issue of this journal, but has not been fully edited. Content may change prior to final publication. Citation information: DOI 10.1109/TVT.2016.2609154, IEEE Transactions on Vehicular Technology

A Framework of Vehicle Trajectory Replanning in Lane Exchanging with Considerations of Driver Characteristics

Jinxiang Wang, Junmin Wang, *Senior Member, IEEE*, and Rongrong Wang, and Chuan Hu

Abstract—This paper presents a control framework to address a typical vehicle-to-vehicle encountering scenario of lane exchanging with two vehicles traveling on contiguous lanes in the same direction and are maneuvered to exchange lanes of each other. A trajectory generating model for lane-changing maneuver is integrated into the driver-vehicle system. Based on this system, both the risk of collision and the lane-exchanging intentions of the drivers can be considered in the trajectory replanning. A linear time-varying model predictive control with parameters of discretized nonlinear system is proposed to realize the optimization objectives of satisfying the drivers' maneuvering intentions and reducing the risk of collision. The optimization problem is subject to the constraints consisting of the human driver preferences, driving habits, and driving capabilities. Simulations have verified the controller's performance and robustness in different scenarios including different initial conditions for the risk of collision and different combinations of drivers' preferences and driving habits. The results show that the proposed controller can satisfy drivers' intentions while avoiding collision in all these scenarios.

***Index Terms*— connected vehicles, collision avoidance, human-vehicle interaction, model predictive control, trajectory replanning, drivers' intention.**

NOMENCLATURE

f, r	Subscripts that denote front and rear, respectively.
p, q	Superscripts that denote young and aged drivers, respectively.
m	Vehicle mass (m).
I_z	Vehicle yaw moment of inertia (kg·m^2).
l_f	Distance of vehicle CG from front axle (m).
l_r	Distance of vehicle CG from rear axle (m).
F_{xi}	Longitudinal tire forces (N) ($i = f, r$).
F_{yi}	Lateral tire forces (N) ($i = f, r$)
V_x	Vehicle longitudinal velocity (m/s).
V_y	Vehicle lateral velocity (m/s).
ψ	Vehicle yaw angle (rad).
C_i	Cornering stiffness (N) ($i = f, r$).
α_i	Slip angle of the tire (rad) ($i = f, r$).
β	Vehicle sideslip angle (rad).
δ_f	Front road wheel steering angle (rad).
δ_{sw}	Steering wheel angle (rad).
a_{xd}	Acceleration/deceleration intention of the driver.
a_{ym}	Maximum vehicle lateral acceleration during the lane-changing maneuver.
Y_{des}, Y	Target and current lateral positions of the vehicle CG, respectively.
G_h	Steering proportional gain.
τ_h	Derivative/lead time constant of the driver's steering (s).
T_h	Lag/delay of the driver's response (s).
R_g	Gear ratio of the steering system.
X_e	Terminal longitudinal position of the vehicle (m)
d_l	Lane width (m).
X	Longitudinal position of the vehicle (m).
ξ	State vector of the system.
u	Input vector of the system
T_s	Sampling time (s).
$\varepsilon_{X,\min}$, $\varepsilon_{Y,\min}$	Minimum longitudinal and lateral safe distances between the two vehicles, respectively (m).
$\varepsilon_{X,th}$, $\varepsilon_{Y,th}$	Thresholds of longitudinal and lateral distances between the two vehicles, respectively (m)
n, σ	Constants in definition of collision threat
κ	Weighting constant.
W_η	Weighting matrix.

J. Wang and R. Wang are with the School of Mechanical Engineering at Southeast University (email: wangjx@seu.edu.cn; wrr06fy@gmail.com).

J. Wang is with Department of Mechanical and Aerospace Engineering at The Ohio State University, Columbus, OH 43210 USA (e-mail: wang.1381@osu.edu).

C. Hu is with the Department of Mechanical Engineering, McMaster University, Hamilton, ON L8S4L8, Canada. (e-mail: huc7@mcmaster.ca).

I. Introduction

ADVANCES in sensory and communication technologies with respect to ground vehicles have recently offered great opportunities for research on semi-automated driver assistance systems. Vehicle states and environmental data including tire-road friction coefficient, lane marks, and information of infrastructures can be acquired by advanced sensing technologies [1][2][3][4]. Information among vehicles, and between vehicles and infrastructure can be communicated as well [5][6]. Among the semi-automated vehicle systems that can share automatic control with human drivers, the safety-oriented advanced driver assistance systems (ADAS) for longitudinal speed control, lane keeping, collision threat detecting/warning, lane changing or overtaking warning applications, and collision avoidance have been intensively studied [7][8][9][10]. Collision-avoidance control systems investigated in the literature mainly concentrate on the modularized longitudinal or lateral collision threat prediction, assessment, and intervention decision making [11][12][13], trajectory/motion planning [14][15], and control algorithms for collision avoidance [9][12][16]. In the literature on threat

0018-9545 (c) 2016 IEEE. Personal use is permitted, but republication/redistribution requires IEEE permission. See http://www.ieee.org/publications_standards/publications/rights/index.html for more information.

This article has been accepted for publication in a future issue of this journal, but has not been fully edited. Content may change prior to final publication. Citation information: DOI 10.1109/TVT.2016.2609154, IEEE Transactions on Vehicular Technology

prediction and collision avoidance, the trajectories of vehicles are assumed to be known in advance and approaches are designed to prevent lane departures [12][16]. In [14][17], the kinodynamic capabilities of vehicle together with other vehicles and road boundaries are considered as constraints for the cooperative motion planning. In [18][19][20][21], the steering command of the driver is shared with the vehicle collision avoidance controller to achieve an optimal control with least intervention against driver's intention. However, other vehicles are treated as static or moving obstacles in these driver assistance controllers without considering cooperative actions among the surrounding vehicles in trajectory planning or controller design.

With the vehicle-to-vehicle (V2V) communications [5], the information on human drivers, vehicles, and environment can be shared among vehicles. The information of a driver may include intentions of steering/throttle/brake operations, and the reaction to variation of the environment. The information of a vehicle can contain the vehicle states such as longitudinal velocity and acceleration, heading angle and yaw rate, vehicle sideslip angle, lateral acceleration, longitudinal and lateral positions. The environmental information of a vehicle would be the tire-road friction coefficient, lane marks, and distances with other vehicles. With the shared information, more sophisticated maneuvers can be implemented instead of merely avoiding collision with vehicles approaching from the opposite direction or traffic moving in the proceeding direction. Because the drivers' intentions, vehicle states, and environment of the involved vehicles can be known, decisions for vehicle trajectory planning, trajectory following, and stability control can be made based on all the shared information, achieving a compromised strategy of trajectory planning for each of the involved vehicles. Some algorithms of cooperative collision avoidance for connected vehicles have been studied recently [14][15].

However, characteristics and satisfactions of the human drivers were seldom considered during trajectory planning in the literature. The characteristics of a human driver include physical limitations such as human time delay, sensory and neuromuscular threshold, and physical attributes such as preview utilization and adaptive control behavior [22]. These characteristics are determined by the immanent driving habits. More details of the analysis, modeling, and identification of human driver behaviors can be found in [22][23][24][25]. If drivers' characteristics and satisfactions are investigated in cooperative controller design for collision avoidance among connected vehicles, both safety and driving comfort can be improved.

To this end, we present a control framework to address a typical V2V encountering scenario of lane exchanging with two vehicles operated by drivers with different characteristics. We assume that the two vehicles in the lane exchanging are within an initial proximity of possible collision. For example, two vehicles traveling on contiguous lanes in the same direction are maneuvered to exchange lanes. If the initial distance between the two vehicles is too close and the two drivers are desired to change lanes simultaneously, risk of collision may arise. The originally desired trajectories of the two vehicles may not be realized for the sake of collision avoidance, and the compromised trajectories should be determined between the two vehicles. We assume that:1) the two vehicles are driven under normal conditions by two drivers with quite different characteristics and driving habits; 2) to reduce the workload of the drivers, we expect that the drivers may intend to conduct the maneuvers of lane-changing regardless of the threat of collision, or the driver overlooks the other vehicle; 3) under assumption 2), the desired/reference trajectories of the drivers can be determined in the scenarios where the drivers encounter with the information of characteristics and behaviors of the drivers [22][26]; and 4) information of vehicle states, environment, and drivers' intentions/preferences can be shared between vehicles.

In order to avoid collision, drivers of the two vehicles may have to take actions to enlarge the distances between them before executing lane changes. There will be many possible options for the drivers to determine when and how to control vehicle speed and steering wheel for safe lane-exchanges. Drivers with different characteristics may come with quite different determinations. The problem then is to find a safe option which satisfies the drivers as much as possible. For such a purpose, this paper designs a trajectory-replanning optimization controller that simultaneously considers the risk of collision, the tracking error of each driver's desired trajectory, and the drivers' characteristics.

Appropriate actions can be taken in advance to diminish the risk of collision, if the longitudinal and lateral distances between the two vehicles in the future can be predicted. Such actions should satisfy multiple objectives including the drivers' intentions and the task of collision avoidance, subject to constraints of vehicle states, environment, and drivers' preferences. Model predictive control (MPC), which has been successfully employed in vehicle stability control, trajectory tracking control and driver-controller shared vehicle collision avoidance [16][18][19][27][28][29], can be applied to address this constrained multi-objective optimization problem. Linear time-varying (LTV) MPC [27] and piecewise affine model based switched MPC [29] are two simplifying approaches to reduce the computational burden of nonlinear MPC in terms of real-time vehicle control applications. Stabilities and effectiveness of these methods have been verified in [29][30].

The contributions of this paper mainly include: 1) An optimization control framework of cooperative trajectory replanning to realize safe lane-exchange is presented, in which preferences and maneuvering intentions of the involved human drivers are considered in the trajectory replanning for collision avoidance; and 2) A LTV MPC with parameters of discretized nonlinear system is proposed to realize the multi-objectives of satisfying the driver maneuvering intentions and reducing collision risk.

The rests of this paper are organized as follows. In Section II the vehicle model, driver model, and trajectory generation model to form the system dynamic model are described. In Section III, the main contributions of this paper, including the control framework, linearization of the system, description of the constraints for risk of collision, and the MPC controller design are presented. In Section IV, simulation results are

0018-9545 (c) 2016 IEEE. Personal use is permitted, but republication/redistribution requires IEEE permission. See http://www.ieee.org/publications_standards/publications/rights/index.html for more information.

This article has been accepted for publication in a future issue of this journal, but has not been fully edited. Content may change prior to final publication. Citation information: DOI 10.1109/TVT.2016.2609154, IEEE Transactions on Vehicular Technology

compared between controllers with different parameters, among scenarios of different initial vehicle positions, and between scenarios of different human driver characteristics. The conclusions are presented in Section V.

II. System Modeling

This section presents the vehicle model, human driver model, and trajectory generation for the controller design. To consider the drivers' intentions in the trajectory replanning for two vehicles in lane exchanging, we integrate these three aspects together to form a nonlinear dynamic system.

To distinguish two drivers with quite different characteristics and driving habits, without loss of generality, we assume there is a *young driver* who prefers to react more aggressively , and an *aged driver* who prefers to react more tardily. That is, the young driver tends to drive with a faster speed, harder acceleration/deceleration, and more rapid steering and accelerating/braking actions, while an aged driver tends to react more modestly with lower vehicle speed, slower steering, and milder acceleration/deceleration. In the following model, the superscript $i = p,q$ is used to represent the two vehicles driven by young and aged drivers, respectively.

A. Vehicle model

A bicycle model, as shown in Fig.1, is used to describe the dynamics of the two vehicles, including longitudinal, yaw, and lateral motions. Assuming that the front tire steering angle is small and without distinguishing the differences in the parameters of the two vehicles, dynamics of the vehicle can be described as

$$m\dot{V}_x^i = mV_y^i\dot{\psi}^i + F_{xf}^i + F_{xr}^i \ , \tag{1}$$

$$m\dot{V}_y^i = -mV_x^i\dot{\psi}^i + F_{yf}^i + F_{yr}^i \ , \tag{2}$$

$$I_z\ddot{\psi}^i = l_f F_{yf}^i - l_r F_{yr}^i \ , \tag{3}$$

where m is vehicle mass, V_x^i and V_y^i are vehicle longitudinal and lateral velocities, respectively. By assuming that the heading angles of the vehicles in lane exchanging is sufficiently small, we have $\cos(\psi^i) \approx 1, \sin(\psi^i) \approx \psi^i$, and then the vehicle motions in the global coordinates can be described as follows,

$$\dot{X}^i = V_x^i - V_y^i\psi^i \ , \tag{4}$$

$$\dot{Y}^i = V_x^i\psi^i + V_y^i \ , \tag{5}$$

where X^i and Y^i are longitudinal and lateral positions of the vehicle along the global coordinates, X and Y, respectively.

The front and rear lateral tire forces can be written as the functions of the tire slip angles described as

$$F_{yf}^i = -2C_f\alpha_f^i, \quad F_{yr}^i = -2C_r\alpha_r^i \ , \tag{6}$$

where C_f and C_r are the front and rear tire cornering stiffness, respectively. The slip angle of the front and rear tires can be calculated as

$$\alpha_f^i = \beta^i + l_f\frac{\dot{\psi}^i}{V_x^i} - \delta_f^i, \quad \alpha_r^i = \beta^i - l_r\frac{\dot{\psi}^i}{V_x^i} \ . \tag{7}$$

Based on the assumption that the vehicle side slip angle is small, we have $\beta^i = V_y^i / V_x^i$.

Neglecting the rolling resistances of the tires, relation between the longitudinal tire forces and the driver's acceleration/ deceleration intention a_{xd}^i can be simply described as follows,

$$ma_{xd}^i = F_{xf}^i + F_{xr}^i. \tag{8}$$

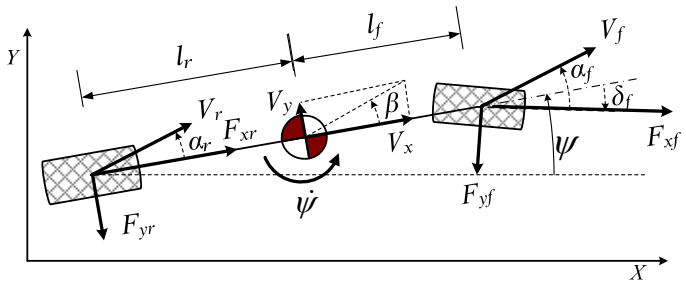

Fig.1. Simplified vehicle "bicycle model".

B. Human Driver Model

In this paper, we integrate the human driver model with the vehicle model to form a closed-loop driver-vehicle system. A comprehensive overview of driver models was given in [24] with respect to different needs of modeling and control applications. A basic driver model is generally regarded as a steering controller to minimize the lateral position deviation between the look-ahead point of the desired path and the predicted position of the vehicle. In this paper, we adopt an approximate driver model introduced by [31], in which the parameters of lead time, delay time and steering proportional gain have been estimated for both young and aged drivers. In this driver model, the applicable steering wheel angle for representing the driver's steering characteristics is described as [31].

$$\delta_{sw}^i = \frac{G_h^i\left(1+\tau_h^i s\right)}{1+T_h^i s}\left(Y_{des}^i - Y^i\right) \ , \tag{9}$$

where Y_{des}^i and Y^i are the target and current lateral positions of the vehicle's center of gravity, G_h^i is the steering proportional gain, τ_h^i is derivative/lead time constant of the driver's steering, T_h^i is time lag/delay of the driver's response, and s is the Laplace operator. These main parameters for describing driver's characteristics, including parameters of young drivers and aged drivers, have been identified in [31] based on the driver model (9). We take these parameters to represent different drivers in this paper. By assuming that the gear ratio of the steering system is R_g , then $\delta_f^i = R_g\delta_{sw}^i$, and the driver model (9) can be rewritten in the form of differential equation,

$$\dot{\delta}_f^i = \frac{-1}{T_h^i}\delta_f^i + \frac{R_g G_h^i}{T_h^i}\left(Y_{des}^i - Y^i\right) + \frac{R_g G_h^i \tau_h^i}{T_h^i}\left(\dot{Y}_{des}^i - V_x^i\psi^i - V_y^i\right) \ . \tag{10}$$

C. Lane-exchanging trajectories generating

The comfort of drivers is related to the maximum lateral acceleration during lane changing or the time elapsed for lane changing [32][33][34]. Under normal operating condition, the vehicle lateral acceleration in lane changing is small. The profile of trajectory and period of time needed for lane changing can be determined by the maximum lateral acceleration allowed during the lane changing maneuver [33], and the trajectory as a

0018-9545 (c) 2016 IEEE. Personal use is permitted, but republication/redistribution requires IEEE permission. See http://www.ieee.org/publications_standards/publications/rights/index.html for more information.

This article has been accepted for publication in a future issue of this journal, but has not been fully edited. Content may change prior to final publication. Citation information: DOI 10.1109/TVT.2016.2609154, IEEE Transactions on Vehicular Technology

function of time is dependent on vehicle speed [32].

In order to generate a differentiable curve for the single lane-changing maneuver, a polynomial trajectory [33] is applied in this paper. By considering vehicles travelling in the same direction on contiguous lanes with the intentions of changing to each other's lane, the desired lane exchanging trajectories of the two vehicles' centers of gravity can be described as

$$Y_{des}^{i}=\begin{cases} d_l\left[10\left(\frac{V_x^i t}{X_e^i}\right)^3-15\left(\frac{V_x^i t}{X_e^i}\right)^4+6\left(\frac{V_x^i t}{X_e^i}\right)^5\right], & i=p \\ d_l\left[1-10\left(\frac{V_x^i t}{X_e^i}\right)^3+15\left(\frac{V_x^i t}{X_e^i}\right)^4-6\left(\frac{V_x^i t}{X_e^i}\right)^5\right], & i=q \end{cases}, \quad (11)$$

where $0\le Y_{des}^{i}\le d_l$, d_l is the lane width, and X_e^i is the terminal longitudinal position of the vehicle, which can be calculated as

$$X_e^i=\frac{V_x^i}{\sqrt{a_{ym}^i}}\sqrt{d_l C_{me}}\ , \quad (12)$$

where a_{ym}^i is the maximum lateral acceleration during the lane-changing maneuver which is always positive, C_{me} is a constant determined by X_e^i and the position where the trajectory curvature is maximum [33].

By assuming that a_{ym}^i is a constant during lane changing, and combining (11) and (12), the desired trajectories for lane-exchanging can be represented as a function of time t,

$$Y_{des}^{i}=\begin{cases} \rho_0\left(\sqrt{a_{ym}^i}t\right)^3+\rho_1\left(\sqrt{a_{ym}^i}t\right)^4+\rho_2\left(\sqrt{a_{ym}^i}t\right)^5, i=p \\ d_l-\rho_0\left(\sqrt{a_{ym}^i}t\right)^3-\rho_1\left(\sqrt{a_{ym}^i}t\right)^4-\rho_2\left(\sqrt{a_{ym}^i}t\right)^5, i=q \end{cases}, \quad (13)$$

where $0\le Y_{des}^{i}\le d_l$, and the three constant coefficients are $\rho_0=\frac{10}{\sqrt{d_l C_{me}^3}}$, $\rho_1=\frac{-15}{d_l C_{me}^2}$, and $\rho_2=\frac{6}{\sqrt{d_l^3 C_{me}^5}}$.

Otherwise, if a_{ym}^i can be adjusted during the lane-exchanging to increase or decrease the duration of maneuver, then (13) is rewritten as

$$Y_{des}^{i}=\begin{cases} \rho_0\left(\int_0^t\sqrt{a_{ym}^i}d\tau\right)^3+\rho_1\left(\int_0^t\sqrt{a_{ym}^i}d\tau\right)^4+\rho_2\left(\int_0^t\sqrt{a_{ym}^i}d\tau\right)^5, i=p \\ d_l-\rho_0\left(\int_0^t\sqrt{a_{ym}^i}d\tau\right)^3-\rho_1\left(\int_0^t\sqrt{a_{ym}^i}d\tau\right)^4-\rho_2\left(\int_0^t\sqrt{a_{ym}^i}d\tau\right)^5, i=q \end{cases}, \quad (14)$$

where $0\le Y_{des}^{i}\le d_l$.

Let d_l =3.66m, by considering two cases with a_{ym}^i =0.5m/s^2 and $a_{ym}^i=0.6-0.5\cos(0.8t)$ m/s^2, respectively, we can obtain the trajectories of the vehicles' centers of gravity generated by (14) as shown in Fig. 2. It can be seen that the trajectories are smooth and differentiable and when a_{ym}^i is small, the lane-exchanging maneuver is mild, when a_{ym}^i increases, the maneuver becomes faster.

By considering the scenario of two vehicles in lane-exchanging, the systems described in (1)–(8), (10), and (14) can be assembled as a path-generating-driver-vehicle system, shown in Fig. 3. By combining two path-generating-driver-vehicle systems, we can define a V2V system for describing two vehicles in the lane exchanging as

$$\dot{\xi}(t)=f\left(\xi(t),u(t)\right), \quad (15)$$

where the state vector of this system consists of the states of the two vehicles, defined as,

$$\xi=\left[V_x^p,V_y^p,\dot{\psi}^p,\delta_f^p,\psi^p,X^p,Y^p,V_x^q,V_y^q,\dot{\psi}^q,\delta_f^q,\psi^q,X^q,Y^q\right]'. \quad (16)$$

The input vector of the system is comprised of the desired longitudinal accelerations and the maximum lateral accelerations of the two vehicles during the lane-exchanging maneuver as

$$u=\left[a_{xd}^p,a_{ym}^p,a_{xd}^q,a_{ym}^q\right]'. \quad (17)$$

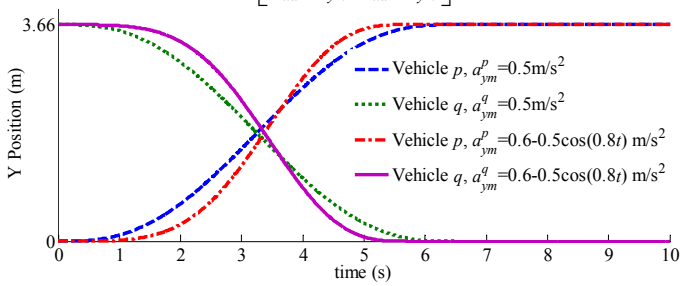

Fig. 2. Lane-exchanging vehicle trajectories.

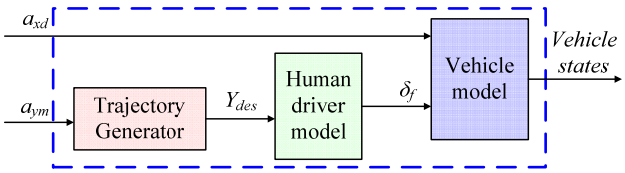

Fig. 3. Structure of the path-generating- driver-vehicle system.

III. CONTROLLER DESIGN

This section firstly presents the description of the control framework, then gives the discretization and linearization of the system proposed in section II and the controller design.

A. Control framework

The trajectory replanning control framework for lane exchanging of two vehicles is described in Fig.4, where intentions of the drivers can be given by the front tire steering angles and throttle/brake inputs. The data of the drivers, including driving habits and preferences, are available in the onboard controllers. The two vehicle reference trajectories representing intentions of the drivers are generated based on these shared data, especially the drivers' preferences of acceleration/deceleration limits as well as the delays of reaction that vary from person to person.

Drivers' desired trajectories of the two vehicles during lane exchanging may conflict each other, and thus the collision will be inevitable if no appropriate action is taken. There are several ways to avoid a collision, either by spacing out in the longitudinal direction by changing vehicle speeds before the maneuver of lane exchanging, or by postponing the maneuvers of lane changing for the two vehicles till safe condition is met. If the drivers' intention satisfactions, drivers' preferences, and safety are all considered, the trajectory planning will become more complicated. These aspects in the trajectory replanning are considered in the MPC-based scheme to achieve the best possible driver intention satisfactions while avoiding collision.

0018-9545 (c) 2016 IEEE. Personal use is permitted, but republication/redistribution requires IEEE permission. See http://www.ieee.org/publications_standards/publications/rights/index.html for more information.

This article has been accepted for publication in a future issue of this journal, but has not been fully edited. Content may change prior to final publication. Citation information: DOI 10.1109/TVT.2016.2609154, IEEE Transactions on Vehicular Technology

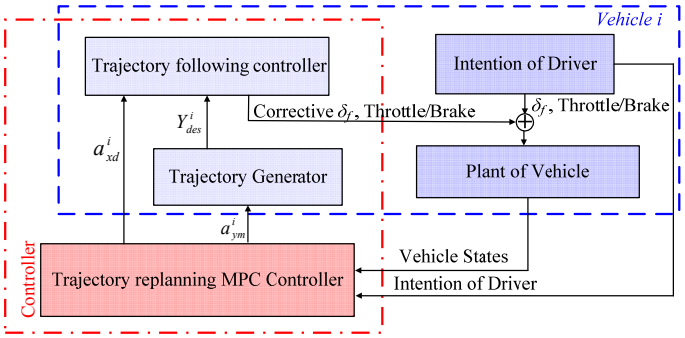

Fig.4. Lane-exchanging vehicle trajectory replanning control framework. Here, i=p, q is used to identify the two vehicle-driver systems, and the trajectory replanning controller are designed to combine and supervise the two vehicles.

This paper focuses on the replanning of the vehicle trajectories during lane exchanging. It is assumed that lower-level trajectory tracking controllers can generate suitable corrective steering and throttle/brake inputs to make the vehicle follow the desired trajectories generated by the proposed controller.

In what follows, for discrete-time systems T_s denotes the sampling time, subscribe k means time kT_s, and subscribe k+j means time $(k+j)T_s$. The superscript $i = p,q$ is used to identify the two vehicles

B. Discretization and linearization

By considering a small sampling time T_s, the system (15) can be discretized and approximated as,

$$\xi_{k+1} = \xi_k + T_s f\left(\xi_k, u_k\right), \tag{18}$$

$$u_k = u_{k-1} + \Delta u_k, \tag{19}$$

where,

$$\xi_k = \left[V^p_{x,k}, V^p_{y,k}, \psi^p_k, \delta^p_{f,k}, \psi^p_k, X^p_k, Y^p_k, V^q_{x,k}, V^q_{y,k}, \dot{\psi}^q_k, \delta^q_{f,k}, \psi^q_k, X^q_k, Y^q_k\right]',$$

$$u_k = \left[a^p_{xd,k}, a^p_{ym,k}, a^q_{xd,k}, a^q_{ym,k}\right]',$$

$$\Delta u_k = \left[\Delta a^p_{xd,k}, \Delta a^p_{ym,k}, \Delta a^q_{xd,k}, \Delta a^q_{ym,k}\right]'.$$

For linearization of the system and MPC design, let k be the current time, ξ_k and u_{k-1} be the current state and previous input respectively, and N be the prediction horizon. At sample time k+j (j=0 ,…, N-1), the nonlinear system (18), (19) can be simplified as

$$\xi_{k+j+1} = \xi_{k+j} + T_s A_{k+j}\xi_{k+j} + g(u_{k+j}), \tag{20}$$

where ξ_{k+j} and u_{k+j} denote the system state and input vectors at sample time k+j of the prediction horizon basing on data at the current time k. A_{k+j} is a matrix calculated at time k+j as

$$A_{k+j} = \begin{bmatrix} A^p_{k+j} & 0 \\ 0 & A^q_{k+j} \end{bmatrix}, \tag{21}$$

where A^i_{k+j} $(i = p,q)$ can be represented as

$$A^i_{k+j} = \begin{bmatrix} 0 & 0 & V^i_{y,k+j} & 0 & 0 & 0 & 0 \\ 0 & \frac{-2(C_f+C_r)}{mV^i_{x,k+j}} & -V^i_{x,k+j}+\frac{2(C_r l_r - C_f l_f)}{mV^i_{x,k+j}} & \frac{2C_f}{m} & 0 & 0 & 0 \\ 0 & \frac{2(C_r l_r - C_f l_f)}{I_z V^i_{x,k+j}} & \frac{-2(C_f l_f^2 + C_r l_r^2)}{I_z V^i_{x,k+j}} & \frac{2C_f l_f}{I_z} & 0 & 0 & 0 \\ 0 & \frac{-R_g G^i_h \tau^i_h}{T^i_h} & 0 & \frac{-1}{T^i_h} & \frac{-R_g G^i_h}{T^i_h}\tau^i_h V^i_{x,k+j} & 0 & \frac{-R_g G^i_h}{T^i_h} \\ 0 & 0 & 1 & 0 & 0 & 0 & 0 \\ 1 & 0 & 0 & 0 & -V^i_{y,k+j} & 0 & 0 \\ 0 & 1 & 0 & 0 & V^i_{x,k+j} & 0 & 0 \end{bmatrix}, \tag{22}$$

where $V^i_{x,k+j}$, $V^i_{y,k+j}$, and ψ^i_{k+j} are values of vehicle states at time k+j.

In (20), $g(u_{k+j})$ is a nonlinear function in terms of the input vector u_{k+j}, described as

$$\begin{cases} g(u_{k+j}) = \begin{bmatrix} g^p(u_{k+j}) & 0 \\ 0 & g^q(u_{k+j}) \end{bmatrix}, \\ g^i(u_{k+j}) = B\left[a^i_{xd,k+j}, \frac{R_g G^i_h}{T^i_h} Y^i_{des}(a^i_{ym,k+j}) + \frac{R_g G^i_h \tau^i_h}{T^i_h} \dot{Y}^i_{des}(a^i_{ym,k+j})\right]', \end{cases} \tag{23}$$

with $i = p,q$, where $a^i_{xd,k+j}$, $a^i_{ym,k+j}$ are values of a^i_{xd}, a^i_{ym} at time k+j respectively, and

$$B = \begin{bmatrix} 1 & 0 & 0 & 0 & 0 & 0 & 0 \\ 0 & 0 & 0 & 1 & 0 & 0 & 0 \end{bmatrix}'.$$

If we define a virtual input vector as

$$\bar{u}_{k+j} = \left[\bar{u}^p_{k+j,0}, \bar{u}^p_{k+j,1}, \ldots, \bar{u}^p_{k+j,5}, \bar{u}^q_{k+j,0}, \bar{u}^q_{k+j,1}, \ldots, \bar{u}^q_{k+j,5}\right]', \tag{24}$$

where elements of $\bar{u}_{k+j}$ are calculated by the elements of u_{k+j} as

$$\begin{cases} \bar{u}^i_{k+j,0} = a^i_{xd,k+j}, \quad i = p,q, \\ \bar{u}^i_{k+j,l} = \left(a^i_{ym,k+j}\right)^{\frac{l}{2}}, \quad i = p,q, \quad l = 1,\ldots,5 \end{cases}, \tag{25}$$

then $g(u_{k+j})$ can be represented by a linear time-varying function in terms of $\bar{u}_{k+j}$ as

$$g\left(u_{k+j}\right) = \bar{g}\left(\bar{u}_{k+j}\right) = \bar{B}_{1,k+j}\bar{u}_{k+j} + \bar{B}_{0,k+j}, \tag{26}$$

where

$$\bar{B}_{1,k+j} = \begin{bmatrix} \bar{B}^p_{1,k+j} & 0 \\ 0 & \bar{B}^q_{1,k+j} \end{bmatrix}, \quad \bar{B}_{0,k+j} = \begin{bmatrix} \bar{B}^p_{0,k+j} \\ \bar{B}^q_{0,k+j} \end{bmatrix}. \tag{27}$$

The matrices in (27) can be described as

$$\bar{B}^i_{1,k+j} = \begin{bmatrix} 1 & 0 & 0 & 0 & 0 & 0 \\ 0 & 0 & 0 & 0 & 0 & 0 \\ 0 & 0 & 0 & 0 & 0 & 0 \\ 0 & \gamma^i_{1,k+j} & \gamma^i_{2,k+j} & \gamma^i_{3,k+j} & \gamma^i_{4,k+j} & \gamma^i_{5,k+j} \\ 0 & 0 & 0 & 0 & 0 & 0 \\ 0 & 0 & 0 & 0 & 0 & 0 \\ 0 & 0 & 0 & 0 & 0 & 0 \end{bmatrix}, \bar{B}^i_{0,k+j} = \begin{bmatrix} 0 \\ 0 \\ 0 \\ \gamma^i_{0,k+j} \\ 0 \\ 0 \\ 0 \end{bmatrix}, \tag{28}$$

where

0018-9545 (c) 2016 IEEE. Personal use is permitted, but republication/redistribution requires IEEE permission. See http://www.ieee.org/publications_standards/publications/rights/index.html for more information.

This article has been accepted for publication in a future issue of this journal, but has not been fully edited. Content may change prior to final publication. Citation information: DOI 10.1109/TVT.2016.2609154, IEEE Transactions on Vehicular Technology

$$\begin{cases}\gamma^p_{l,k+j}=\dfrac{R_gG^p_h}{T^p_h}P^p_{l,k+j}+\dfrac{R_gG^p_h\tau^p_h}{T^p_h}\bar{P}^p_{l,k+j}, l=1,\ldots,5,\\ \gamma^q_{l,k+j}=-\dfrac{R_gG^q_h}{T^q_h}P^q_{l,k+j}-\dfrac{R_gG^q_h\tau^q_h}{T^q_h}\bar{P}^q_{l,k+j}, l=1,\ldots,5,\\ \gamma^p_{0,k+j}=\dfrac{R_gG^p_h}{T^p_h}P^p_{0,k+j},\\ \gamma^q_{0,k+j}=d_l-\dfrac{R_gG^q_h}{T^q_h}P^q_{0,k+j}.\end{cases}$$

The procedures for linearization of $g(u_{k+j})$ and the derivation of (26) through (28) can be found in Appendix A.

In order to reduce the burden of computation, we expect the matrices A^i_{k+j}, $\bar{B}_{1,k+j}$, and $\bar{B}_{0,k+j}$ remain un-updated over the prediction horizon. By replacing $V^i_{x,k+j}$, $V^i_{y,k+j}$, and ψ^i_{k+j} with $V^i_{x,k}$, $V^i_{y,k}$, and ψ^i_k, respectively, A_{k+j} is replaced by matrix A_k, which is calculated at current time k and remained invariant during the prediction horizon. Similarly, by replacing z^i_{k+j} with z^i_k, $\bar{B}_{1,k+j}$ and $\bar{B}_{0,k+j}$ are replaced by matrices $\bar{B}_{1,k}$ and $\bar{B}_{0,k}$ respectively, which are also calculated at time k and remain invariant during the prediction horizon. Stability analysis for this method of simplification can be found in [30].

C. Constraints of collision avoidance

Under normal driving condition, the time for lane-changing maneuver is not very small, i.e., maximum lateral acceleration during lane change is not large, such that the maximum variation of vehicle heading angle during lane changing is small. Safe distance between the two vehicles to avoid collision can be represented by safe distances along both longitudinal and lateral coordinates as follows,

$$\left|X^p_k-X^q_k\right|\geq\varepsilon_{X,\min},\ \left|Y^p_k-Y^q_k\right|\geq\varepsilon_{Y,\min},\qquad(29)$$

where X^i_k, Y^i_k denote longitudinal and lateral positions of the two vehicles at sample time k respectively, $\varepsilon_{X,\min}$ and $\varepsilon_{Y,\min}$ are the minimum longitudinal and lateral safe distances respectively. By employing the hyperbolic tangent function $\tanh(x)=(e^x-e^{-x})/(e^x+e^{-x})$, the hard constraint defined by (29) can be described as threat of collision between the two vehicles defined as follows,

$$h(\varepsilon_{X,k},\varepsilon_{Y,k})=\frac{1}{\left(2+\tanh\left(\sigma\left(\dfrac{\varepsilon^2_{X,k}}{\varepsilon^2_{X,th}}-1\right)\right)+\tanh\left(\sigma\left(\dfrac{\varepsilon^2_{Y,k}}{\varepsilon^2_{Y,th}}-1\right)\right)\right)^n},\qquad(30)$$

where $\varepsilon_{X,k}=\left|X^p_k-X^q_k\right|$, $\varepsilon_{Y,k}=\left|Y^p_k-Y^q_k\right|$, $\varepsilon_{X,th}$ and $\varepsilon_{Y,th}$ are thresholds of the longitudinal and lateral distances between the two vehicles, which are designed a little larger than $\varepsilon_{X,\min}$ and $\varepsilon_{Y,\min}$, respectively. In (30), n is a constant positive integer, σ is a positive constant. These constants can be adjusted to change the shape of function $h(\varepsilon_{X,k,t},\varepsilon_{Y,k,t})$ and to tune the influence of the constraint.

In (30), $\varepsilon^2_{X,k},\varepsilon^2_{Y,k}\in[0,+\infty)$, and $\forall x\in(-\infty,+\infty)$, $\tanh(x)\in(-1,1)$ is a monotonically increasing function. Such that $h(\varepsilon_{X,k},\varepsilon_{Y,k})$ is also monotonic and has a fixed upper bound $1/(2+2\tanh(-\sigma))^n$, which is a positive constant. The partial differentials of $h(\varepsilon_{X,k},\varepsilon_{Y,k})$ with respect to $\varepsilon^2_{X,k}$ and $\varepsilon^2_{Y,k}$ are both negative. This means that $h(\varepsilon_{X,k},\varepsilon_{Y,k})$ is monotonically decreasing with respect to distance between the two vehicles.

To further describe the characteristics of $h(\varepsilon_{X,k},\varepsilon_{Y,k})$ and the determination of parameters in (30), a 3-D graph based on (30) is drawn with safe distance thresholds of $\varepsilon_{X,th}=8.5$m, $\varepsilon_{Y,th}=3.4$m, and suitable constants n=6, $\sigma=2$, as shown in Fig. 5.

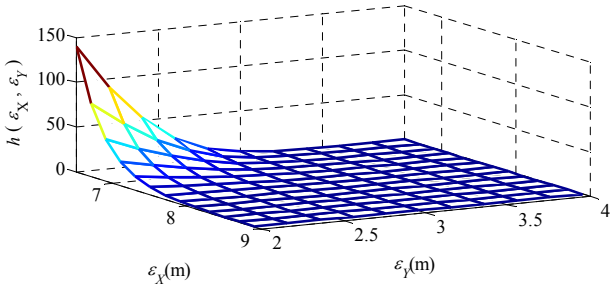

Fig. 5. The threat of collision between the lane-exchanging vehicles. ε_X and ε_Y describe the longitudinal and lateral distances between the two vehicles respectively, and $h(\varepsilon_X,\varepsilon_Y)$ is threat of collision between the two vehicles.

Remark 1: The criteria of tuning n and σ are described as: 1) when the distances are around $\varepsilon_{X,th}$ or $\varepsilon_{Y,th}$, the value of $h(\varepsilon_{X,k},\varepsilon_{Y,k})$ increases gradually with decreasing distances; 2) when the distances become smaller, the value of $h(\varepsilon_{X,k},\varepsilon_{Y,k})$ increases sharply, for the sake of representation of collision threat. The partial differential values of $h(\varepsilon_{X,k},\varepsilon_{Y,k})$ with respect to $\varepsilon_{X,k}$ and $\varepsilon_{Y,k}$ are designed to be mild around $\varepsilon_{X,th}$ and $\varepsilon_{Y,th}$, for the sake of computing feasibility of the optimal problem considering this threat of collision.

D. MPC controller design

The task of the MPC controller is to make optimal decision of trajectory replanning, by which intentions and preferences of the two drivers are satisfied optimally within the constraints of collision avoidance and actuator limits.

By assuming that during the scenario of lane exchanging the drivers have their own intentions of vehicle velocities and required durations for lane changing maneuvers, determination of the required lane changing time can be represented by the profiles of trajectories and the response of yaw rates. That is, the combination of tracking desired vehicle velocities, yaw rates, and lateral trajectories can be applied as the control objective of the MPC controller. Meanwhile the constraint of collision avoidance can be represented as minimizing the maximum threat of collision between the two vehicles over the prediction horizon. Therefore, this constraint can be soften and included in the cost function of the MPC controller.

Provided with the vehicle states ξ_k at current time k and the previous system virtual input $\bar{u}_{k-1}$, the optimization problem to be solved in the receding horizon is defined as follows,

0018-9545 (c) 2016 IEEE. Personal use is permitted, but republication/redistribution requires IEEE permission. See http://www.ieee.org/publications_standards/publications/rights/index.html for more information.

This article has been accepted for publication in a future issue of this journal, but has not been fully edited. Content may change prior to final publication. Citation information: DOI 10.1109/TVT.2016.2609154, IEEE Transactions on Vehicular Technology

$$\min_{\Delta U_k}\left\{\sum_{j=0}^{N-1}\left\|W_\eta\left(\eta_{k+j}-\eta_{ref,k+j}\right)\right\|^2+\max_{j=0}^{N-1}\left[\kappa h\left(\varepsilon_{X,k+j},\varepsilon_{Y,k+j}\right)\right]\right\}, \quad (31a)$$

$$\text{s.t.}\quad \xi_{k+j+1,t}=\left(I+T_sA_k\right)\xi_{k+j}+\bar{B}_{1,k}\bar{u}_{k+j}+\bar{B}_{0,k},\quad j=0,...,N-1, \quad (31b)$$

$$\eta_{k+j}=\begin{bmatrix}\Phi & 0\\ 0 & \Phi\end{bmatrix}\xi_{k+j},\Phi=\begin{bmatrix}1&0&0&0&0&0&0\\0&0&1&0&0&0&0\\0&0&0&0&0&0&1\end{bmatrix},\ j=0,...,N-1, \quad (31c)$$

$$\bar{u}_{k+j}=\bar{u}_{k+j-1}+\Delta\bar{u}_{k+j},\quad j=0,...,N-1, \quad (31d)$$

$$\bar{u}_{k-1}=\bar{u}((k-1)T_s), \quad (31e)$$

$$\xi_k=\xi\left(kT_s\right), \quad (31f)$$

$$\bar{u}_{\min}\le\bar{u}_{k+j}\le\bar{u}_{\max},\quad j=0,...,N-1, \quad (31g)$$

$$\Delta\bar{u}_{\min}\le\Delta\bar{u}_{k+j}\le\Delta\bar{u}_{\max},\quad j=0,...,N-1, \quad (31h)$$

$$\bar{u}_{k+j}=\left[\bar{u}^p_{k+j,0},...,\bar{u}^p_{k,5},\bar{u}^q_{k+j,0},...,\bar{u}^q_{k+j,5}\right]',j=0,...,N-1, \quad (31i)$$

$$\Delta\bar{u}_{k+j}=\left[\Delta\bar{u}^p_{k+j,0},...,\Delta\bar{u}^p_{k,5},\Delta\bar{u}^q_{k+j,0},...,\Delta\bar{u}^q_{k+j,5}\right]',j=0,...,N-1, \quad (31j)$$

$$\bar{u}^i_{k+j,l}=\left(\bar{u}^i_{k+j,1}\right)^l,\quad i=p,q,\quad l=2,...5,\quad j=0,...,N-1. \quad (31k)$$

In (31a), ΔU_k is defined as the incremental sequence of input vectors over the prediction horizon $\left[\Delta\bar{u}_k,...,\Delta\bar{u}_{k+N-1}\right]'$. W_η is a diagonal matrix denoting the weights of longitudinal velocities, yaw rates, and lateral trajectories of the two vehicles. $\eta_{ref,k+j}=\left[V^p_{x,ref,k+j},\dot{\psi}^p_{ref,k+j},Y^p_{ref,k+j},V^q_{x,ref,k+j},\dot{\psi}^q_{ref,k+j},Y^q_{ref,k+j}\right]'$ is the reference states of the two vehicles consisting of desired longitudinal velocities, yaw rates, and lateral trajectories generated by the nonlinear model (15) with the initial reference inputs of the two drivers. The second term of (31a) represents the soften constraint of collision avoidance, described by the maximum threat of collision over the prediction horizon. $h(\varepsilon_{X,k+j},\varepsilon_{Y,k+j})$ is defined by (30). κ is a constant to scale influence of the maximum collision threat to be large enough when the value of $h(\varepsilon_{X,k+j},\varepsilon_{Y,k+j})$ becomes nonzero over the prediction horizon.

In (31b), I is a 14x14 identity matrix. A_k, $\bar{B}_{1,k}$, and $\bar{B}_{0,k}$ remain invariant over the prediction horizon for reducing the burden of computation.

In order to calculate lower and upper bounds of the virtual input vector, $\bar{u}_{\min}$ and $\bar{u}_{\max}$ in (31g), we define

$$\begin{cases}u_{\min}=\left[a^p_{xd,\min},a^p_{ym,\min},a^q_{xd,\min},a^q_{ym,\min}\right]',\\ u_{\max}=\left[a^p_{xd,\max},a^p_{ym,\max},a^q_{xd,\max},a^q_{ym,\max}\right]',\end{cases} \quad (32)$$

which are known lower and upper bounds of the real input vector, respectively. We define $\bar{u}_{\min}$ and $\bar{u}_{\max}$ as,

$$\begin{cases}\bar{u}_{\min}=\left[\bar{u}^p_{\min,0},\bar{u}^p_{\min,1},...,\bar{u}^p_{\min,5},\bar{u}^q_{\min,0},\bar{u}^q_{\min,1},...,\bar{u}^q_{\min,5}\right]',\\ \bar{u}_{\max}=\left[\bar{u}^p_{\max,0},\bar{u}^p_{\max,1},...,\bar{u}^p_{\max,5},\bar{u}^q_{\max,0},\bar{u}^q_{\max,1},...,\bar{u}^q_{\max,5}\right]',\end{cases} \quad (33)$$

then elements of the virtual input bounds can be calculated as

$$\begin{cases}\bar{u}^i_{\min,0}=a^i_{xd,\min},\ \bar{u}^i_{\max,0}=a^i_{xd,\max},\ i=p,q,\\ \bar{u}^i_{\min,l}=\left(a^i_{ym,\min}\right)^{\frac{l}{2}},\ \bar{u}^i_{\max,l}=\left(a^i_{ym,\max}\right)^{\frac{l}{2}},\ l=1,...,5,\ i=p,q.\end{cases} \quad (34)$$

By using (31d), constraint (31g) can be converted into inequality constraints for $\Delta\bar{u}_{k+j}$ as follows,

$$\begin{cases}\sum_{l=0}^{j}\Delta\bar{u}_{k+l}\le\bar{u}_{\max}-\bar{u}_{k-1},j=0,...,N-1,\\ -\sum_{l=0}^{j}\Delta\bar{u}_{k+l}\le\bar{u}_{k-1}-\bar{u}_{\min},j=0,...,N-1.\end{cases} \quad (35)$$

$\bar{u}_{k-1}$ is invariant over the prediction horizon, such that the right hand sides of the inequalities are invariant.

In order to calculate the rate limits of the virtual input, $\Delta\bar{u}_{\min}$ and $\Delta\bar{u}_{\max}$ in (31h), we define

$$\begin{cases}\Delta u_{\min}=\left[\Delta a^p_{xd,\min},\Delta a^p_{ym,\min},\Delta a^q_{xd,\min},\Delta a^q_{ym,\min}\right]',\\ \Delta u_{\max}=\left[\Delta a^p_{xd,\max},\Delta a^p_{ym,\max},\Delta a^q_{xd,\max},\Delta a^q_{ym,\max}\right]',\end{cases} \quad (36)$$

which are the known lower and upper bounds of deviations of the real inputs between two consecutive sample times. Then we can calculate $\Delta\bar{u}_{\min}$ and $\Delta\bar{u}_{\max}$ with the method similar to (33) and (34).

Constraint (31j) is derived from (25) to describe the interdependency among elements of the virtual input vector.

The sequence of optimal virtual input deviations is denoted by $\Delta U^*_k=\left[\Delta\bar{u}^*_k,...,\Delta\bar{u}^*_{k+N-1}\right]'$, which is computed at current time k by solving (31a) through (31k) for the current state ξ_k and previous input $\bar{u}_{k-1}$. The first sample of ΔU^*_k, i.e., $\Delta\bar{u}^*_k$, is added to the previous input $\bar{u}((k-1)T_s)$. The resultant $\bar{u}(kT_s)$ is applied to calculate commands of the desired lateral trajectories and longitudinal accelerations/decelerations for the two vehicles. At the next control time sample k+1, $\xi(kT_s)$ and $\bar{u}((k-1)T_s)$ are updated by $\xi((k+1)T_s)$ and $\bar{u}(kT_s)$ respectively in calculating the initial condition and coefficients, with which the optimization problem (31a) through (31k) is solved.

Remark 2: With the constraint (31b), trajectories of the two vehicles are confined in the two adjacent lanes, i.e., the vehicles will be restricted within the boundaries of the double lanes if they are able to follow the paths defined by (31b). On the other hand, the value of $h(\varepsilon_{X,k},\varepsilon_{Y,k})$ increases sharply with the decreasing distance between the two vehicles when the initial distance is smaller than the threshold. If there are only two vehicles and without obstacles in the lanes, and κ in (31a) is large enough, the maximum threat of collision over the prediction horizon should be very small to achieve the optimal solution for the MPC controller. In this way, a safe distance between the two vehicles is guaranteed, as can be deduced by definition (30) or Fig. 5 with a very small threat of collision. Furthermore, the maximum lateral accelerations of the two vehicles in lane-changing are bounded by constraint (31g), such that the handling stability for the two vehicles are guaranteed. To sum up, stable lane-exchanging maneuvers to avoid collision can be achieved with the proposed MPC controller.

Remark 3: If there are other vehicles or static obstacles in the lanes, additional constraints acting as the environmental envelope introduced in [18] can be added into the MPC controller. These additional constraints might conflict with the lane-exchanging paths confined by (31b), which means the lane exchanging cannot be realized in the given environment.

Remark 4: The personal characteristics or driving habits of drivers are described with the differences of the lower and upper

0018-9545 (c) 2016 IEEE. Personal use is permitted, but republication/redistribution requires IEEE permission. See http://www.ieee.org/publications_standards/publications/rights/index.html for more information.

This article has been accepted for publication in a future issue of this journal, but has not been fully edited. Content may change prior to final publication. Citation information: DOI 10.1109/TVT.2016.2609154, IEEE Transactions on Vehicular Technology

bounds of longitudinal and lateral accelerations and their rate limits in constraints (31g) and (31h). The characteristics of the drivers are also represented by the parameters of lead/lag time and steering gain of the driver model, being included in constraint (31b). In the system model, initial reference inputs of the two drivers are the nominal longitudinal accelerations and maximum lateral accelerations during lane-changing. Since the drivers may intend to change lane regardless of the threat of collision, their intentions can be reflected by the nominal vehicle states $\eta_{ref,k+j}$ generated by the system model with these initial reference inputs.

Remark 5: Although (31b) is an LTV system with invariant parameters over the prediction horizon, constraint (31k) and the soften distance constraint are nonlinear. Therefore problem (31a) through (31k) cannot be reduced to a standard quadratic programming (QP) problem. We employ the constrained nonlinear optimization algorithm [35] to convert this problem into an unconstrained optimization problem.

IV. SIMULATION RESULTS

In this section, simulations are conducted to verify the effectiveness of the proposed trajectory replanning controller under the conditions of different initial threads of collision and with vehicles driven by different drivers.

The MPC controller in Section III-D is implemented to determine the lane exchanging trajectories for the two vehicles which are driven on contiguous lanes in the same direction. We assume that the parameters and road condition of the two vehicles are identical. The two vehicles are driven by a young driver and an aged driver, respectively, and they both decide to make lane change simultaneously.

A 10-DOF nonlinear vehicle model is applied as the controlled plant in simulation. This vehicle model consists of three degrees of translational freedom of vehicle body, three degrees of rational freedom, and the rotational motion for each of the four tires. The Dugoff's tire model is adopted to calculate the longitudinal and lateral tire-road friction forces. Model parameters of the two vehicles in simulation are identical. Details of the model and parameters can be found in [36].

Parameters describing the preferences and driving habits for the young and aged drivers are list as follows. Among these parameters, steering proportional gain, driver delay time and lead time (representing the look-ahead preview time) for young and aged drivers are taken from [31].

- For the young driver, $T_h^p=0.13$s , $G_h^p=0.8$, $\tau_h^p=1.1$, $a_{xd,\min}^p=-4\text{m/s}^2$, $a_{xd,\max}^p=3\text{m/s}^2$, $a_{ym,\min}^p=0.1\text{m/s}^2$, $a_{ym,\max}^p=4\text{m/s}^2$, $\Delta a_{xd,\min}^p=-0.2\text{m/s}^2$, $\Delta a_{xd,\max}^p=0.2\text{m/s}^2$, $\Delta a_{ym,\min}^p=-0.25\text{m/s}^2$, $\Delta a_{ym,\max}^p=0.25\text{m/s}^2$.
- For the aged driver, $T_h^q=0.18$s , $G_h^q=0.5$, $\tau_h^q=1.1$, $a_{xd,\min}^q=-3\text{m/s}^2$, $a_{xd,\max}^q=2\text{m/s}^2$, $a_{ym,\min}^q=0.05\text{m/s}^2$, $a_{ym,\max}^q=2.5\text{m/s}^2$, $\Delta a_{xd,\min}^q=-0.15\text{m/s}^2$, $\Delta a_{xd,\max}^q=0.15\text{m/s}^2$, $\Delta a_{ym,\min}^q=-0.2\text{m/s}^2$, $\Delta a_{ym,\max}^q=0.2\text{m/s}^2$.

The simulations are implemented in the environment of Matlab/Simuink. We use the optimization toolbox *fmincon* in Matlab to find the optimum of the constrained optimal problem.Parameters of the MPC controller are presented as follows,

Sample time $T_s=0.05$s , horizon $N=24$; in (31a), the weighting diagonal matrix $W_\eta\in\mathbb{R}^{6\times6}$, with $W_{\eta11}=W_{\eta44}=1$, $W_{\eta22}=W_{\eta55}=10$, $W_{\eta33}=W_{\eta66}=100$, and weight for the soften constraint $\kappa=100$; in(30), $\varepsilon_{X,th}=8.5\text{m}$, $\varepsilon_{Y,th}=3.4\text{m}$, n=6, $\sigma=2$.

A. Lane exchange of vehicles with different initial distances

In this section two scenarios with different initial distances between the two vehicles are simulated. Both of the scenarios are facing the threat of collision.

Initial states for the two vehicles and initial inputs for the controllers are as follows.

- The initial value of X^q is 0 m. The initial value of X^p is set to be 0 m in Scenario I and 4 m in Scenario II. That means the relative initial longitudinal distances between the two vehicles are 0 m and 4 m in Scenario I and Scenario II, respectively, with which the threat of collision exists. Initial value of Y^p and Y^q are 0m and 3.66m, respectively. The other initial states of the two vehicles are zeros.
- The initial virtual input vector of the MPC controller is $\Delta\bar{u}(0)=\bar{u}(0)=[0,0,0,0,0,0,0,0,0,0,0,0]'$.

The reference inputs for the two vehicles throughout the simulation are given as $u_{ref}(t)=[0.2,0.8,0,0.4]'\ \text{m/s}^2$. With the reference inputs, the vehicle driven by the young driver has an intention of a longitudinal acceleration as $0.2\ \text{m/s}^2$, while the vehicle driven by the aged driver maintains a constant velocity. The maximum lateral acceleration of the vehicle driven by the young driver is 0.8m/s^2 , larger than that of vehicle driven by the aged driver. The reference states of the two vehicles are generated by nonlinear model (15) with the reference inputs.

Simulation results of the two scenarios are compared in Fig. 6 through Fig. 11. It can be seen in Fig. 6 and Fig. 7 that, at about 0.6 s in scenario I and 0.4 s in scenario II, the soften constraint of the collision avoidance has been activated. The value of a_{xd}^p has been increased while a_{xd}^q decreased, resulting in a fact that Vehicle *p* has been speeded up while Vehicle *p* is slowed down as described in Fig. 8. It is shown in Fig. 7 (b) that a_{ym}^q has been reduced to or remains at its lower bound with the intention to delay the lane changing maneuver for Vehicle *q*. This delay action of Vehicle *p* does not last so long as Vehicle *q*, as shown in Fig. 7 (a). These modifications of accelerations are all constrained by their upper and lower bounds. The control effect of modifications on a_{ym}^p and a_{ym}^q can be seen in Fig. 10, where the lane changing maneuvers have been delayed, and the lateral trajectories of the controlled vehicles have been changed. These results show that, in order to diminish the future threat of collision, the decision has been made to increase the longitudinal distance between the two vehicles before the lateral distance between them becomes too small.

0018-9545 (c) 2016 IEEE. Personal use is permitted, but republication/redistribution requires IEEE permission. See http://www.ieee.org/publications_standards/publications/rights/index.html for more information.

This article has been accepted for publication in a future issue of this journal, but has not been fully edited. Content may change prior to final publication. Citation information: DOI 10.1109/TVT.2016.2609154, IEEE Transactions on Vehicular Technology

Fig. 11 is drawn for depicting the real-time trajectories of the two vehicles in lane exchanging. In Fig. 11, small solid rectangles and solid triangles denote the center positions of Vehicle p and Vehicle q respectively, the 7 m long by 2 m wide large rectangles represent profiles of the vehicles. The positions of the two vehicles at the same instants of time are connected by dash lines with double arrows. It can be seen clearly in Fig. 11, the vehicles have not been collided in both scenarios.

As compared with the results in Section IV–A, the tracking errors of vehicle states including velocities, yaw rates, and the trajectories are larger in the two scenarios of this section. And the closer the initial distance is, the more critical the future threat of collision will be. Such that actions to avoid collision are taken with larger amplitudes or with longer time of duration, as can be seen in Fig. 6 and Fig. 7. It is shown in Fig. 8 through Fig. 10 that the tracking errors of Scenario I are larger than those of Scenario II during lane exchange. The maximum velocity tracking error of Vehicle p is 4.52 m/s in Scenario I compared with 2.72 m/s in Scenario II, and this error of Vehicle q is 5.02 m/s in Scenario I compared with 2.27 m/s in Scenario II. In Scenario II, the vehicle trajectories can follow their references with maximum lateral position errors of 0.24 m for Vehicle p and 0.16 m for Vehicle q. In Scenario I, the tracking errors of yaw rates and trajectories are much larger than those in Scenario II. The reason of these differences can be explained as in Scenario I the threat of collision is much more critical and the controller emphasizes more on reducing this threat than on decreasing the tracking errors. Therefore, a_{ym}^{p} and a_{ym}^{q} in Scenario I have been reduced and maintained at their lower bounds for longer time than those in Scenario II.

Nevertheless, after lane exchange both the velocities and lateral trajectories of the vehicles can be tracked perfectly in the two scenarios presented in this section, as soon as the threat of collision has been relieved.

As comparing the desired acceleration inputs and responses of the vehicles driven by the young and aged drivers in scenario I, we can find some differences due to different intentions, driving habits, and preferences between the two drivers. As shown in Fig. 6 and Fig. 8, velocity of Vehicle p increases while velocity of Vehicle q decreases during lane change. This result is in favor of minimizing the cost function, as acceleration of Vehicle p is expected to be 0.2 m/s^2, while Vehicle q is not expected to be accelerated. As shown in Fig. 7, in Scenario I, from beginning a_{ym}^{q} has been maintained at its lower bound for a long time. However, a_{ym}^{p} has not remained at its lower bound for so long. These differences lead to quite different trajectories of the two vehicles, as shown in Fig. 10.

More details of the comparison can be found in TABLE I, where the main variables of trajectory following and collision avoidance for the two scenarios are listed. In TABLE I, both maximum trajectory errors and the root mean squared trajectory errors of the vehicle states are given. The starting time of changing vehicle velocities to increase the longitudinal distance, and the starting time of delaying lane changing maneuvers are presented for comparison. The time when the longitudinal distance reach the safe threshold, and the lateral distance at this time are presented to explicate how the collision avoidance is realized.

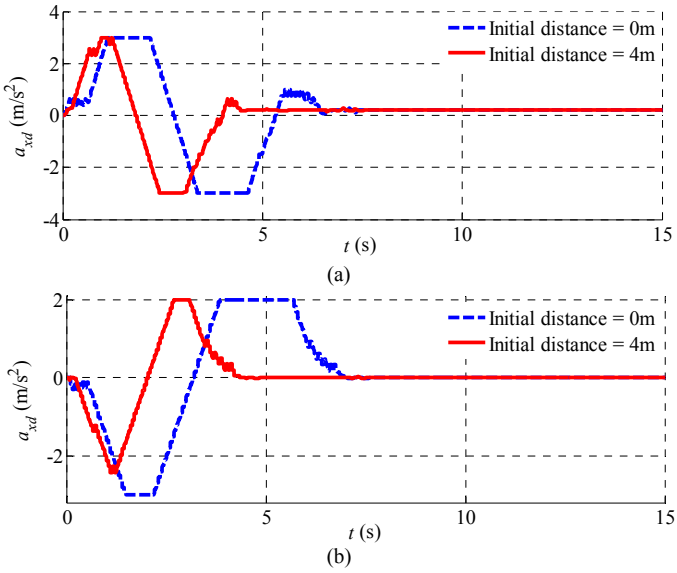

Fig. 6. Desired longitudinal accelerations of the vehicles with different initial longitudinal distances: (a) vehicle p driven by young driver, (b) vehicle q driven by aged driver.

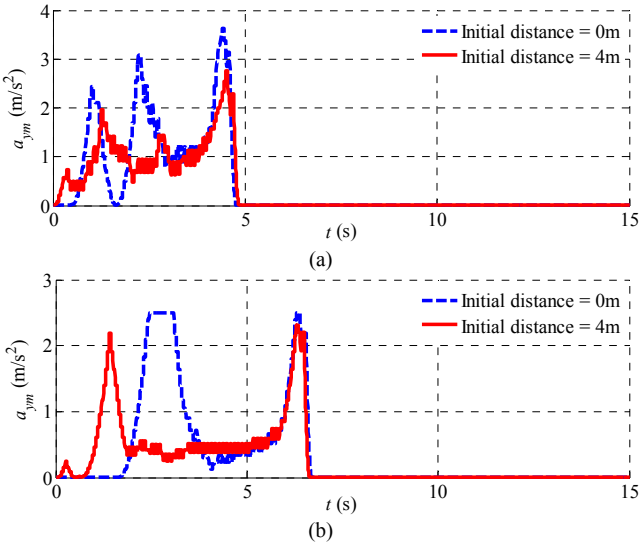

Fig. 7. The maximum lateral accelerations during the lane change of the vehicles with different initial longitudinal distances: (a) value the Vehicle p driven by young driver, (b) value of the Vehicle q driven by aged driver.

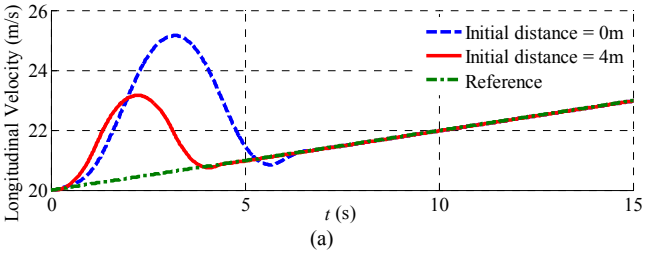

0018-9545 (c) 2016 IEEE. Personal use is permitted, but republication/redistribution requires IEEE permission. See http://www.ieee.org/publications_standards/publications/rights/index.html for more information.

This article has been accepted for publication in a future issue of this journal, but has not been fully edited. Content may change prior to final publication. Citation information: DOI 10.1109/TVT.2016.2609154, IEEE Transactions on Vehicular Technology

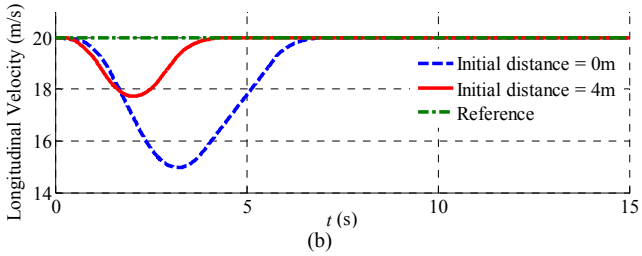

(b)

Fig. 8. Longitudinal velocities of the vehicles with different initial longitudinal distances:(a) vehicle p driven by young driver, (b) vehicle q driven by aged driver.

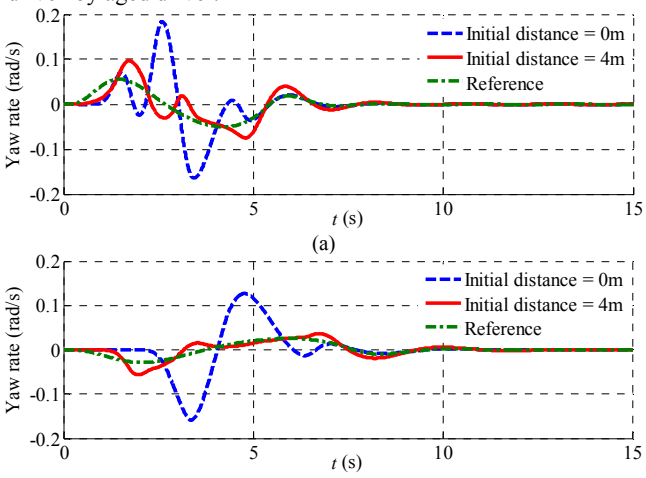

(a)

(b)

Fig. 9. Yaw rate responses of the vehicles with different initial longitudinal distances: (a) Vehicle p driven by young driver, (b) Vehicle q driven by aged driver.

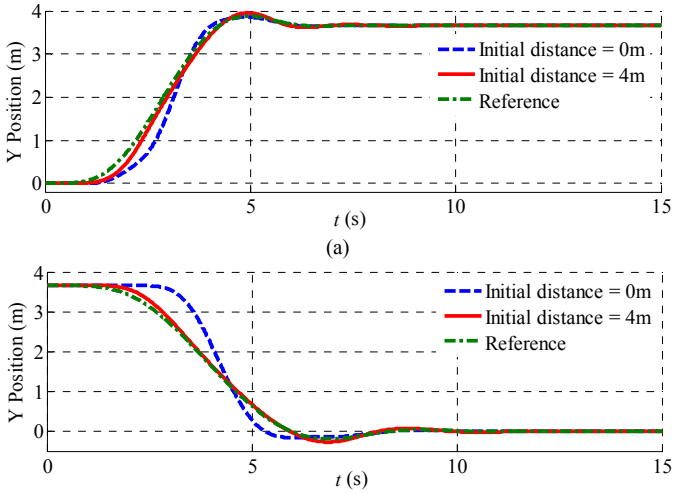

(a)

(b)

Fig. 10. Y Positions responses of the vehicles' centers of gravity with different initial longitudinal distances:: (a) vehicle p driven by young driver, (b) vehicle q driven by aged driver.

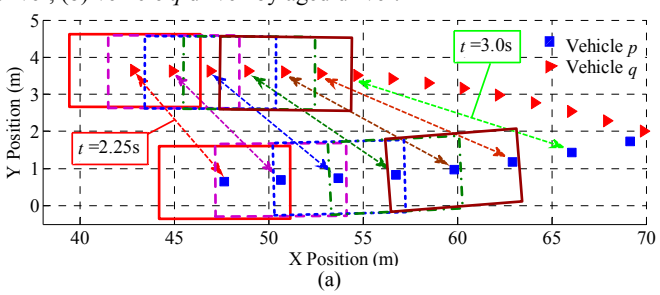

(a)

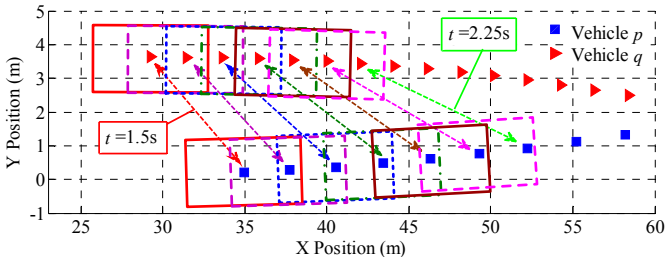

(b)

Fig. 11. Trajectories of vehicles with different longitudinal distances: (a) with initial distances of 0m, (b) with initial distances of 4m.

TABLE I

COMPARISON OF SIMULATION RESULTS AMONG THE VEHICLES WITH DIFFERENT INITIAL LONGITUDINAL DISTANCES

	Initial distance	$\Delta V_{x\max}$ (m/s)	$\Delta r_{\max}$ (rad/s)	$\Delta Y_{\max}$ (m)	$\Delta r_{\rm rms}$ (rad/s)	$\Delta Y_{\rm rms}$ (10^{-3}m)	T_{vc} (s)	T_{dlc} (s)	T_{th} (s)	ε_{Yth} (m)
Vehicle p	0m	4.52	0.180	0.717	7.3×10^{-4}	3.4	0.15	--	2.62	2.77
	4m	2.72	0.046	0.243	2.7×10^{-4}	1.4	0.30	0.50	2.00	3.07
Vehicle q	0m	5.02	0.151	0.937	7.6×10^{-4}	5.2	0.15	--	2.62	2.77
	4m	2.27	0.028	0.160	1.5×10^{-4}	0.96	0.30	0.35	2.00	3.07

$\Delta r_{\rm rms}$ and $\Delta Y_{\rm rms}$ are the root mean squared (rms) tracking errors of yaw rate and Y position, respectively. $\Delta V_{x\max}$, $\Delta r_{\max}$, and $\Delta Y_{\max}$ are maximum tracking error of longitudinal velocity, yaw rate, and Y position, respectively. T_{vc} is starting time of changing velocities of the vehicles to increase the longitudinal distance. T_{dlc} is starting time of delaying lane changing maneuver. T_{th} is the time when the longitudinal distance between two vehicles hits the threshold distance. ε_{Yth} is the lateral distance between the two vehicles at time T_{th} .

B. Lane exchange of vehicles driven by both young drivers

In this section we present simulation results of two vehicles driven by two young drivers, respectively. In this scenario, the parameters describing the preferences and driving habits for the driver of Vehicle p remain unchanged as those of young driver in the previous simulation. And parameters for the driver of Vehicle q are changed to those of young driver as well. The MPC controller parameters are identical as Section IV–A. Both the initial values of X^p and X^q are set to be 0m, and other initial values of the vehicle states and the initial inputs of MPC controller are identical as those in Section IV–A. In order to diminish the difference between the two vehicles, the reference inputs of the two vehicles are set to be $u_{ref}(t) = [0.2, 0.8, 0.2, 0.8]'$.

The simulation results are shown in Fig. 12 and Fig. 13. It is shown in Fig. 12 (a) and (b), Vehicle p is chosen to slow down while Vehicle q is chosen to speed up, for increasing distance between the two vehicles. Both of a_{ym}^p and a_{ym}^q have been maintained at their lower bound to delay lane-changing maneuvers for the two vehicles, as shown in Fig. 12 (a). It can be seen in Fig. 12 (b), (c), and (d) that states of the vehicles cannot follow their references well during lane change due to the efforts of avoiding collision. And there are some differences between tracking errors of the two vehicles because of their difference in longitudinal velocities during lane change. Fig. 13 shows that the two vehicles can successfully avoid collision. Both vehicles can track their references well after lane exchange, when the threat of collision has been removed.

More details of the simulation results are list in TABLE II, in which it is clear that the actions taken by the two drivers almost happen simultaneously, and lateral trajectory tracking

0018-9545 (c) 2016 IEEE. Personal use is permitted, but republication/redistribution requires IEEE permission. See http://www.ieee.org/publications_standards/publications/rights/index.html for more information.

This article has been accepted for publication in a future issue of this journal, but has not been fully edited. Content may change prior to final publication. Citation information: DOI 10.1109/TVT.2016.2609154, IEEE Transactions on Vehicular Technology

errors of the two vehicles are with little difference.

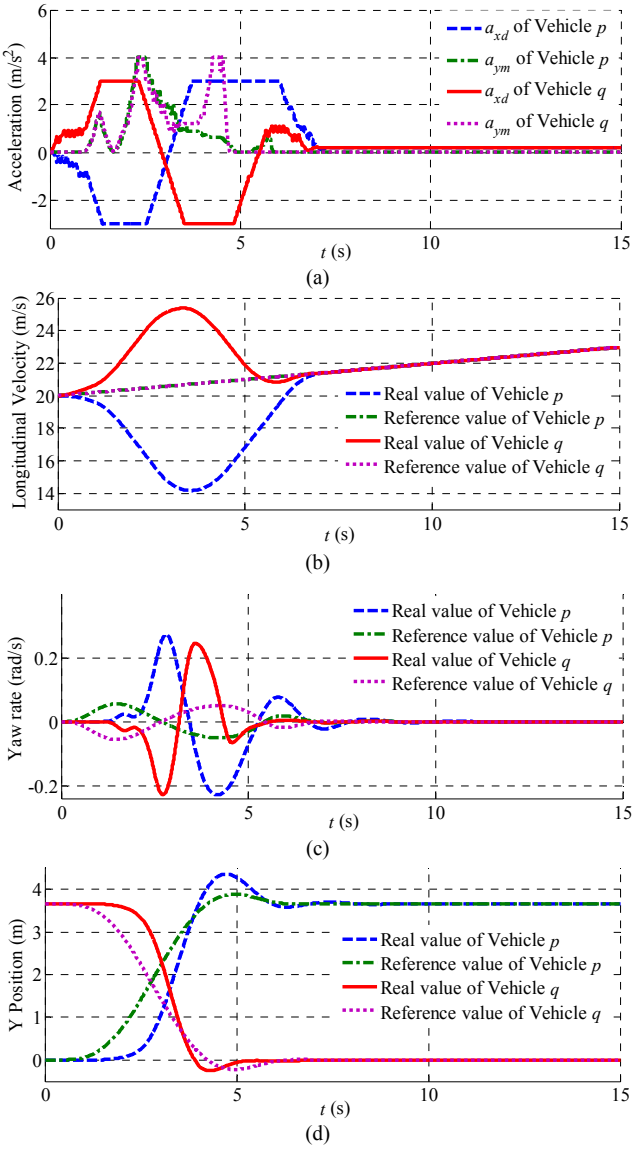

Fig. 12. Desired accelerations and states of the vehicles driven by two young drivers: (a) desired longitudinal acceleration and maximum lateral acceleration of the vehicles during lane changing, (b) Longitudinal velocity of the vehicles, (c) Yaw rate response of the vehicles, (d) Y Positions response of the vehicles.

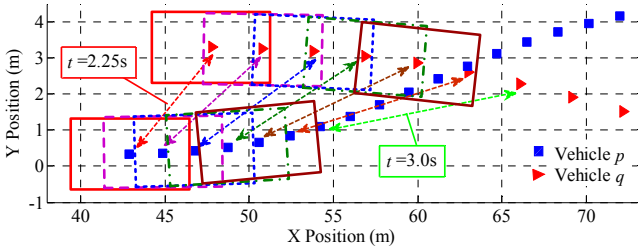

Fig. 13. Trajectories of the vehicles driven by two young drivers.

TABLE II
SIMULATION RESULTS OF THE VEHICLES DRIVEN BY BOTH YOUNG DRIVERS

	$\Delta V_{x\max}$ (m/s)	$\Delta r_{\max}$ (rad/s)	$\Delta Y_{\max}$ (m)	$\Delta r_{\rm rms}$ (rad/s)	$\Delta Y_{\rm rms}$ (10^{-3}m)	T_{vc} (s)	T_{lh} (s)	ε_{Yth} (m)
Vehicle p	6.55	0.280	1.27	1.3×10^{-3}	6.7	0.15	2.65	2.76
Vehicle q	4.72	0.231	1.14	1.1×10^{-3}	5.5	0.15	2.65	2.76

The nomenclatures are defined the same as in Table I

The comparisons of several lane-exchanging scenarios with different risks of collision have illustrated that the proposed controller can deal with the multiple objectives of tracking drivers' intentions and avoiding collision with different threat of collision simultaneously. Comparisons of scenarios for vehicles driven by two young drivers and by young and aged drivers have verified that the proposed controller can appropriately handle situations involving different human drivers.

V. CONCLUSIONS

In this paper, a controller of trajectory replanning for semi-automated vehicle systems lane-exchanging situation is presented. A polynomial trajectory generating model for lane-changing maneuver has been integrated into the driver-vehicle system to form a V2V system for trajectory replanning. Based on this V2V system, both risk of collision and intentions of the drivers described by desired vehicle states are considered for trajectory replanning in different scenarios of lane exchange. A MPC controller is proposed to realize the optimization of multiple objectives including the satisfaction of the drivers' intentions and collision avoidance. In the controller, the preferences, driving habits, and the abilities of the drivers are considered as constraints. The constraints of collision avoidance have been soften by introducing a function derived from the hyperbolic tangent function. The tracking errors of the drivers' intentions described by vehicle longitudinal velocities, yaw rates, and lateral positions have been considered as costs in the optimization. Simulation results indicate that the proposed controller can appropriately tradeoff the multiple objectives for tracking drivers' intention and avoiding collision, with different threats of collisions and vehicles driven by different drivers.

APPENDIX A

The following section presents the linearization of $g^i(u_{k+j})$. Y^i_{des} and $\dot{Y}^i_{des}$ in (23) are not easy to be linearized because they must satisfy the lane-exchanging trajectories described by (14), which is nonlinear in terms of a^i_{ym}.

Let z^i_{k+j} be the value of $\int_0^t \sqrt{a^i_{ym}}d\tau$ at time $k+j$. Then by assuming that z^i_k has been calculated using the history of a^i_{ym}, the update function of the desired lateral trajectory Y^i_{des} over the prediction horizon can be derived from (14) and described as

$$\begin{cases} Y^p_{des,k+j+1} = \rho_0\left(z^p_{k+j+1}\right)^3 + \rho_1\left(z^p_{k+j+1}\right)^4 + \rho_2\left(z^p_{k+j+1}\right)^5, \\ Y^q_{des,k+j+1} = d_l - \rho_0\left(z^q_{k+j+1}\right)^3 - \rho_1\left(z^q_{k+j+1}\right)^4 - \rho_2\left(z^q_{k+j+1}\right)^5, \\ z^i_{k+j+1} = z^i_{k+j} + T_s\sqrt{a^i_{ym,k+j}}, \quad i = p,q, \end{cases} \tag{A1}$$

with j=0,…,N-1, where $Y^i_{des,k+j+1}$ and z^i_{k+j+1} are values of the desired vehicle lateral position and $\int_0^t \sqrt{a^i_{ym}}d\tau$ at time $k+j+1$, respectively.

The update function (A1) can be rewritten by the polynomial form in terms of $\left(a^i_{ym,k+j}\right)^{\frac{1}{2}}$ as follows,

0018-9545 (c) 2016 IEEE. Personal use is permitted, but republication/redistribution requires IEEE permission. See http://www.ieee.org/publications_standards/publications/rights/index.html for more information.

This article has been accepted for publication in a future issue of this journal, but has not been fully edited. Content may change prior to final publication. Citation information: DOI 10.1109/TVT.2016.2609154, IEEE Transactions on Vehicular Technology

$$\begin{cases} Y^p_{des,k+j+1} = P^p_{0,k+j} + \sum_{l=1}^{5} P^p_{l,k+j} \left(a^i_{ym,k+j}\right)^{\frac{l}{2}}, \\ Y^q_{des,k+j+1} = d_l - P^q_{0,k+j} - \sum_{l=1}^{5} P^q_{l,k+j} \left(a^q_{ym,k+j}\right)^{\frac{l}{2}}, \end{cases} \tag{A2}$$

where $P^i_{l,k+j}, l = 0,...,5$ are determined at time $k+j$ as,

$$\begin{cases} P^i_{0,k+j} = \rho_0 \left(z^i_{k+j}\right)^3 + \rho_1 \left(z^i_{k+j}\right)^4 + \rho_2 \left(z^i_{k+j}\right)^5, \\ P^i_{1,k+j} = 3\rho_0 T_s \left(z^i_{k+j}\right)^2 + 4\rho_1 T_s \left(z^i_{k+j}\right)^3 + 5\rho_2 T_s \left(z^i_{k+j}\right)^4, \\ P^i_{2,k+j} = 3\rho_0 T_s^2 z^i_{k+j} + 6\rho_1 T_s^2 \left(z^i_{k+j}\right)^2 + 10\rho_2 T_s^2 \left(z^i_{k+j}\right)^3, \\ P^i_{3,k+j} = \rho_0 T_s^3 + 4\rho_1 T_s^3 z^i_{k+j} + 10\rho_2 T_s^3 \left(z^i_{k+j}\right)^2, \\ P^i_{4,k+j} = \rho_1 T_s^4 + 5\rho_2 T_s^4 z^i_{k+j}, \\ P^i_{5,k+j} = \rho_2 T_s^5. \end{cases} \tag{A3}$$

In order to calculate the value of $\dot{Y}^i_{des}$ at time $k+j+1$, by considering a small T_s, we use the approximate finite difference form as

$$\frac{\Delta Y^i_{des,k+j+1}}{T_s} = \frac{Y^i_{des,k+j+1} - Y^i_{des,k+j}}{T_s}. \tag{A4}$$

By substituting (A2) into (A4) and reorganizing the outcome to be the polynomial form of $\left(a^i_{ym,k+j}\right)^{\frac{1}{2}}$, we can find

$$\begin{cases} \Delta Y^p_{des,k+j+1} = T_s \sum_{l=1}^{5} \overline{P}^p_{l,k+j} \left(a^p_{ym,k+j}\right)^{\frac{l}{2}}, \\ \Delta Y^q_{des,k+j+1} = -T_s \sum_{l=1}^{5} \overline{P}^q_{l,k+j} \left(a^q_{ym,k+j}\right)^{\frac{l}{2}}, \end{cases} \tag{A5}$$

where $\overline{P}^i_{l,k+j}, l = 1,...,5$ are determined at time $k+j$ as,

$$\begin{cases} \overline{P}^i_{1,k+j} = 3\rho_0 \left(z^i_{k+j}\right)^2 + 4\rho_1 \left(z^i_{k+j}\right)^3 + 5\rho_2 \left(z^i_{k+j}\right)^4, \\ \overline{P}^i_{2,k+j} = 3\rho_0 T_s z^i_{k+j} + 6\rho_1 T_s \left(z^i_{k+j}\right)^2 + 10\rho_2 T_s \left(z^i_{k+j}\right)^3, \\ \overline{P}^i_{3,k+j} = \rho_0 T_s^2 + 4\rho_1 T_s^2 z^i_{k+j} + 10\rho_2 T_s^2 \left(z^i_{k+j}\right)^2, \\ \overline{P}^i_{4,k+j} = \rho_1 T_s^3 + 5\rho_2 T_s^3 z^i_{k+j}, \\ \overline{P}^i_{5,k+j} = \rho_2 T_s^4. \end{cases} \tag{A6}$$

By simplifying $\dot{Y}^i_{des}$ with the finite difference form (A4), we have

$$\begin{cases} \dot{Y}^p_{des,k+j+1} = \sum_{l=1}^{5} \overline{P}^p_{l,k+j} \left(a^p_{ym,k+j}\right)^{\frac{l}{2}}, \\ \dot{Y}^q_{des,k+j+1} = -\sum_{l=1}^{5} \overline{P}^q_{l,k+j} \left(a^q_{ym,k+j}\right)^{\frac{l}{2}}, \end{cases} \tag{A7}$$

Given the value of z^i_k, $g^i(u_{k+j})$ can be updated by using (A2) and (A7). Obviously, $g^i(u_{k+j})$ cannot be simplified as linear function of u_{k+j}.

If we define a virtual input vector $\overline{u}_{k+j}$ given by (24) with the transfer function (25) from the real system input vector u_{k+j}, then by substituting (A2), (A7), (24) and (25) into (23), $g(u_{k+j})$ can be represented as a linear time-varying function as described by (26) through (28).

REFERENCES

[1] R. Rajamani, G. Phanomchoeng, D. Piyabongkarn, J. Y. Lew, "Algorithms for real-time estimation of individual wheel tire-road friction coefficients," *IEEE/ASME Trans. Mechatronics*, vol. 17, no. 6, pp. 1183-1195, Dec. 2012.

[2] J. Wang, L. Alexander, and R. Rajamani, "Friction estimation on highway vehicles using longitudinal measurements," ASME J. Dyn. Syst., Meas., Control, vol. 126, no. 2, pp. 265–275, Jun. 2004.

[3] D. I. Randeniya, S. Sarkar, M. Gunaratne, "Vision–IMU integration using a Slow-Frame-Rate monocular vision system in an actual roadway setting," *IEEE Trans. Intell. Transp. Syst.,* vol. 11, no. 2, pp. 256-266, Jun. 2010.

[4] P. Y. Shinzato , V. Grassi, F. S. Osório, D. F. Wolf, "Fast visual road recognition and horizon detection using multiple artificial neural networks," *in Proc. IEEE Intelligent Vehicles Symposium*, 2012, pp. 1090-1095.

[5] J. Gozálvez, M. Sepulcre, R. Bauza, "IEEE 802.11 p vehicle to infrastructure communications in urban environments," *IEEE Commun. Mag.*, vol. 50, no.5, pp. 176-183, May. 2012.

[6] B. Gallagher, H. Akatsuka, H. Suzuki, "Wireless communications for vehicle safety: Radio link performance and wireless connectivity methods," *IEEE Veh. Technol. Mag.*, vol. 1, no. 4, pp. 4–24, Dec. 2006.

[7] M. Lu, K. Wevers, R. Van Der Heijden, "Technical feasibility of advanced driver assistance systems (ADAS) for road traffic safety," *Transport. Plan. Techn.,* vol. 28, no.3, pp. 167-187, 2005.

[8] C. Maag, D. Muhlbacher, C. Mark, H. P. Kruger, "Studying effects of advanced driver assistance systems (ADAS) on individual and group level using multi-driver simulation," *IEEE Intell. Transp. Syst. Mag.*, vol. 4, no. 3, pp. 45-54, Fall 2012.

[9] R. Isermann, R. Mannale, K. Schmitt, "Collision-avoidance systems PRORETA: Situation analysis and intervention control," *Control Eng. Pract.*, vol. 20, no.11, pp. 1236-1246, Nov. 2012.

[10] M. Sepulcre, J. Gozalvez, "Experimental evaluation of cooperative active safety applications based on V2V communications," *in Proc. the ninth ACM international workshop on Vehicular inter-networking, systems, and applications*, 2012, pp. 13-20.

[11] P. Falcone, M. Ali, J. Sjoberg, "Predictive threat assessment via reachability analysis and set invariance theory," *IEEE Trans. Intell. Transp. Syst.*, vol. 12, no. 4, pp. 1352-1361, Dec. 2011.

[12] A. Gray, M. Ali, Y. Gao, J. K. Hedrick, F. Borrelli, "A Unified Approach to Threat Assessment and Control for Automotive Active Safety," *IEEE Trans. Intell. Transp. Syst.*, vol. 14, no.3, pp.1490-1499, Sept. 2013.

[13] M. Brannstrom, F. Sandblom, L. Hammarstrand, "A probabilistic framework for decision-making in collision avoidance systems," *IEEE Trans. Intell. Transp. Syst.*, vol. 14, no. 2, pp. 637-648, Jun. 2013.

[14] C. Frese and J. Beyerer, "A comparison of motion planning algorithms for cooperative collision avoidance of multiple cognitive automobiles," *in Proc. IEEE Intell. Veh. Symp*., Jun. 2011, pp. 1156–1162.

[15] M. Hafner, D. Cunningham, L. Caminiti, and D. Del Vecchio, "Cooperative collision avoidance at intersections: Algorithms and experiments," *IEEE Trans. Intell. Transp. Syst*., vol. 14, no. 3, pp. 1162–1175, Sep. 2013.

[16] M. Ali, P. Falcone, C. Olsson, J. Sjoberg, "Predictive Prevention of Loss of Vehicle Control for Roadway Departure Avoidance," *IEEE Trans. Intell. Transp. Syst.*, vol. 14, no.1, pp. 56-68, Mar. 2013.

[17] J. B. Tomas-Gabarron, E. Egea-Lopez, J. Garcia-Haro, "Vehicular trajectory optimization for Cooperative Collision Avoidance at high speeds". *IEEE Trans. Intell. Transp. Syst.*, vol. 14, no.4, pp. 1930-1941, Dec. 2013.

[18] S. Erlien, S. Fujita, J. C. Gerdes, "Safe driving envelopes for shared control of ground vehicles". *in 7th IFAC Symposium on Advances in Automotive Control*, Sept. 2013, vol. 7, no. 1, pp. 831-836.

[19] S. J. Anderson, S. B. Karumanchi, K. Iagnemma, "Constraint-based planning and control for safe, semi-autonomous operation of vehicles", *in IEEE Intelligent Vehicles Symposium*, Jun. 2012, pp. 383-388.

[20] X. Na, D. J. Cole, "Game-Theoretic Modeling of the Steering Interaction Between a Human Driver and a Vehicle Collision Avoidance Controller", *IEEE Transactions on Human-Machine Systems*, vol. 45, no.1, pp. 25-38, Feb. 2015.

[21] J. Wang, G. Zhang, R. Wang, S. Schnelle, and J. Wang, "A Gain-Scheduling Driver Assistance Trajectory Following Algorithm Considering Different Driver Steering Characteristics," *IEEE Transactions on Intelligent Transportation Systems* (in press), 2016 (DOI: 10.1109/TITS.2016.2598792).

[22] C. C. Macadam, "Understanding and modeling the human driver", *Vehicle Syst. Dyn.*, vol. 40, nos. 1-3, pp. 101-134, 2003.

[23] A. J. Pick, D. J. Cole, "A mathematical model of driver steering control including neuromuscular dynamics," *Trans. ASME, J. Dyn. Syst., Meas., Control*, vol. 130, no. 3, p. 031004, May 2008.

0018-9545 (c) 2016 IEEE. Personal use is permitted, but republication/redistribution requires IEEE permission. See http://www.ieee.org/publications_standards/publications/rights/index.html for more information.

This article has been accepted for publication in a future issue of this journal, but has not been fully edited. Content may change prior to final publication. Citation information: DOI 10.1109/TVT.2016.2609154, IEEE Transactions on Vehicular Technology

[24] M. Plöchl, J. Edelmann, "Driver models in automobile dynamics application," *Vehicle Syst. Dyn.*, vol. 45, nos. 7-8, pp. 699–741, Jul. 2007.

[25] J. Steen, H. J. Damveld, R. Happee, M. M. van Paassen, and M. Mulder, "A review of visual driver models for system identification purposes," *in IEEE International Conf. on Systems, Man, and Cybernetics (SMC)*, 2011, pp. 2093 – 2100.

[26] D. Salvucci, "Modeling driver behavior in a cognitive architecture," *Hum. Factors*, vol. 48, no. 2, pp. 362–380, 2006.

[27] P. Falcone, F. Borrelli, J. Asgari, H. E.Tseng, D. Hrovat, "Predictive active steering control for autonomous vehicle systems," *IEEE Trans. Control Syst. Technol.*, vol. 15, no.3, pp. 566-580, May 2007.

[28] C. E. Beal, J. C. Gerdes, "Model Predictive Control for Vehicle Stabilization at the Limits of Handling," *EEE Trans. Control Syst. Technol.*, vol. 21, no. 4, pp. 1258-1269, Jul. 2013.

[29] S. Di Cairano, H. E. Tseng, D. Bernardini, A. Bemporad. "Vehicle yaw stability control by coordinated active front steering and differential braking in the tire sideslip angles domain," *EEE Trans. Control Syst. Technol.*, vol. 21, No.4, pp. 1236-1248. Jul. 2013

[30] P. Falcone, F. Borrelli, H. E. Tseng, J. Asgari, D. Hrovat, "Linear time-varying model predictive control and its application to active steering systems: Stability analysis and experimental validation," *Int. J. Robust Nonlinear Control*, vol. 18, no.8, pp. 862-875, May 2008.

[31] Y. W. Chai, Y. Abe, Y. Kano, M. Abe, "A study on adaptation of SBW parameters to individual driver's steer characteristics for improved driver–vehicle system performance," *Vehicle System Dynamics*, vol. 44, no.sup1, pp. 874-882, 2006.

[32] I. Papadimitriou, M. Tomizuka, "Fast lane changing computations using polynomials," *in Proc. the IEEE American Control Conference*, 2003, Vol. 1, pp. 48-53.

[33] W. Chee, M. Tomizuka, (1994, Oct.) Vehicle Lane Change Maneuver in Automated Highway Systems. California Partners Adv. Transit Highways, Berkley, CA, PATH Research Report, UCB-ITS-PRR-94-22. [Online]. Available: http://escholarship.org /uc/ item/29j5s3gk.

[34] G. Xu, L. Liu, Y. Ou, Z. Song, "Dynamic modeling of driver control strategy of lane-change behavior and trajectory planning for collision prediction," *IEEE Trans. Intell. Transp. Syst.*, vol. 13, no.3, pp. 1138-1155, Sept. 2012.

[35] M. S. Bazaraa, H. D. Sherali, C. M. Shetty. "Penalty and barrier functions," *Nonlinear programming: theory and algorithms*, 3rd ed., John Wiley & Sons, pp. 469–535, 2006.

[36] J. Wang, N. Chen, D. Pi, G. Yin, "Agent-based coordination framework for integrated vehicle chassis control," *Proceedings of the IMechE., Part D: Journal of Automobile Engineering*, vol. 223, no.5, pp. 601-621, May 2009.

0018-9545 (c) 2016 IEEE. Personal use is permitted, but republication/redistribution requires IEEE permission. See http://www.ieee.org/publications_standards/publications/rights/index.html for more information.